

UNCLASSIFIED
**Optimum Communication and Surveillance Frequencies
for Atmospheric Reentry Vehicles**

Paul Christopher
Odyssey Systems Consulting Group
1800 Diagonal Rd, Alexandria, VA 22314
pfchristop@aol.com

(U) Abstract

We show general refractive indices and attenuation for reentry plasma as a function of frequency and altitude. Peng's stagnation plasma observations then allow us to show attenuation as a function of altitude and velocity. Specific reentry trajectories, as a Shuttle trajectory, are applied to find plasma attenuation as a function of altitude. Extremely high UHF attenuation is shown and low Ka band attenuation is indicated. Frequencies higher than 30 GHz are also attractive, but must include higher atmospheric attenuation. Further surveillance advantages are indicated for the 26-45 and 75-98 GHz regions. We indicate the broadband Chirp capabilities of radar at frequencies greater than 30 GHz.

1. Background

Vehicles reentering the earth's atmosphere at high altitudes induce a shock wave. The plasma in the shock wave causes immediate communication concerns: these concerns have been recognized since the early '60s (1). Frank Dirsra recommended that reentry communications be shifted to frequencies higher than UHF. His recommendations were not followed, and critical vehicles such as Apollo 13 suffered extensive blackouts on reentry. Pressing schedules and budgets kept UHF in service, and questions about "best" communication frequencies remained relatively untreated.

We develop a general index of refraction equation for plasma, based on Davies (2). We apply it to atmospheric reentry profiles (3) which show characteristic velocities as a function of altitude during reentry. Classical plasma attenuation is then found with the aid of the molecular mean free path as a function of altitude (4). We show attenuation for a low earth altitude reentry vehicle for UHF frequencies. High attenuation is indicated for low frequencies in the 90 to 105 km altitude regime. Large improvements are found at higher frequencies through Ka band, and we show the large improvements to be expected at 26 GHz. The wide range of frequencies considered requires both classical attenuation and quantum tunneling effects, and we extend the classical results to quantum tunneling results with the aid of Dendy (5) and Schiff (6). These plots can be an aid in choosing reentry profiles to avoid large plasma attenuation.

We indicate sharply improved communication results for Ku band in the 12-14 GHz range. Plasma attenuation is further indicated to drop to low values at 26 GHz. Optimum frequencies appear approximately in the 26-45 GHz and 75-98 GHz regions.

Surveillance frequencies would also benefit from these millimeter wave considerations. Lower frequencies, such as UHF, would retain their value in the search mode. They should however be aware of any sudden increase in radar cross section for targets below 110 km altitude. That would be a signal for millimeter wave radars in the 26-45 or 75-98 GHz region to closely track the target during reentry.

UNCLASSIFIED

UNCLASSIFIED

BEST AVAILABLE COPY

2. Analysis

The reentry vehicle typically noses up before its altitude drops below 110 km. This resultant drag allows massive energy to be dissipated before the high pressure regions of the atmosphere are encountered. A plasma layer (shock layer) forms at the nose and extends as an envelope around the vehicle.

We start the attenuation and refraction studies associated with the plasma layer with a close look at the index of refraction of the plasma and its relation to classical attenuation. We

develop an extension of Davies' index of refraction (Appendix).

The stagnation plasma density has been found by Peng (7) from Cornell Aeronautical Lab experiments. It is applied as $fn2$ in the Appendix. The data may be presented as a function of altitude and velocity as Fig. 2-1. Mathematica (8) is helpful for Fig. 2-1 and 2-2. The plasma density (Fig 2-1) can be related to the angular plasma frequency (Appendix) as Fig. 2-2.

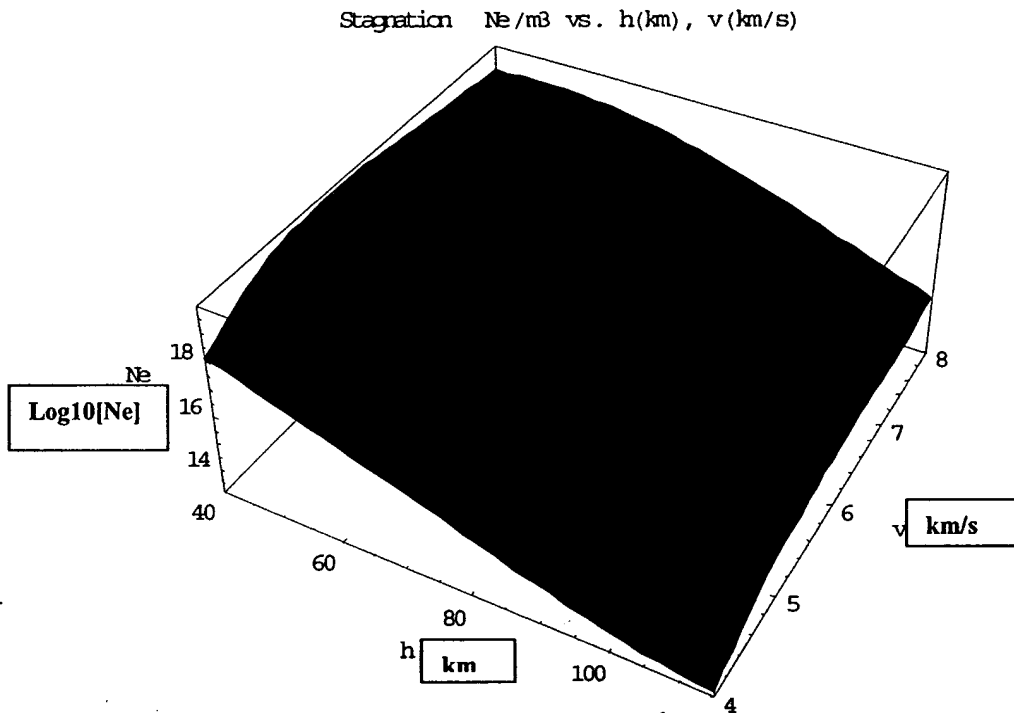


Fig. 2-1 Peng's Plasma Density (Electrons/ m^3) v. Altitude (km), V (km/s)
Pgm PengAug03b.nb

UNCLASSIFIED

UNCLASSIFIED

Peng's Stagnation ω_p (rad/s) vs. h, v

BEST AVAILABLE COPY

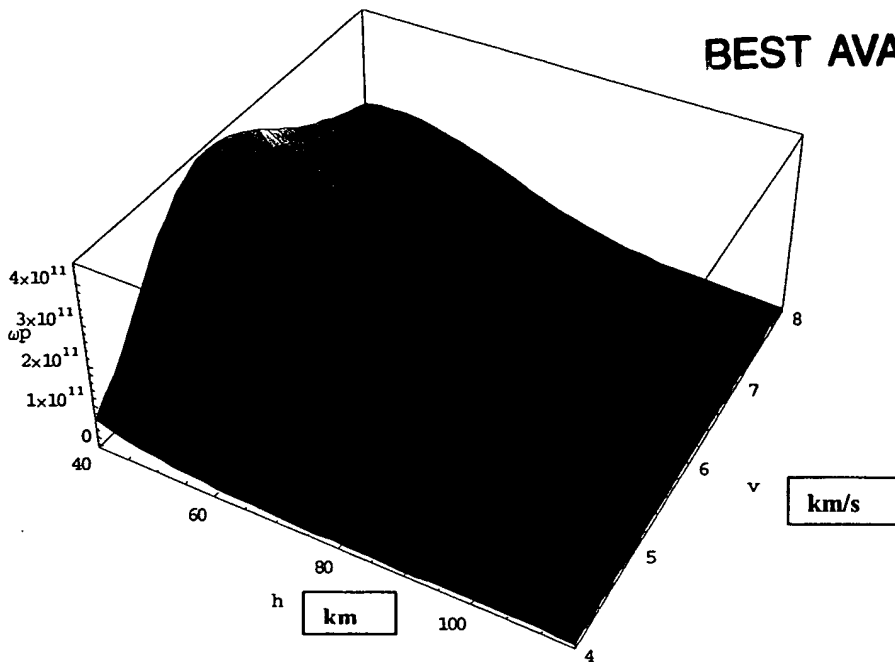


Fig. 2-2 Angular Plasma Frequency Corresponding to Peng's Plasma Density

UHF Communication and Surveillance

With the above results, we will now be able to see why overwhelming attenuation occurs at UHF frequencies. Fig. 2-3 shows the index of

refraction near zero for broad parts of the reentry altitude, indicating a strongly reflecting layer at 60 - 110 km altitude.

Index of Refraction vs. h, v

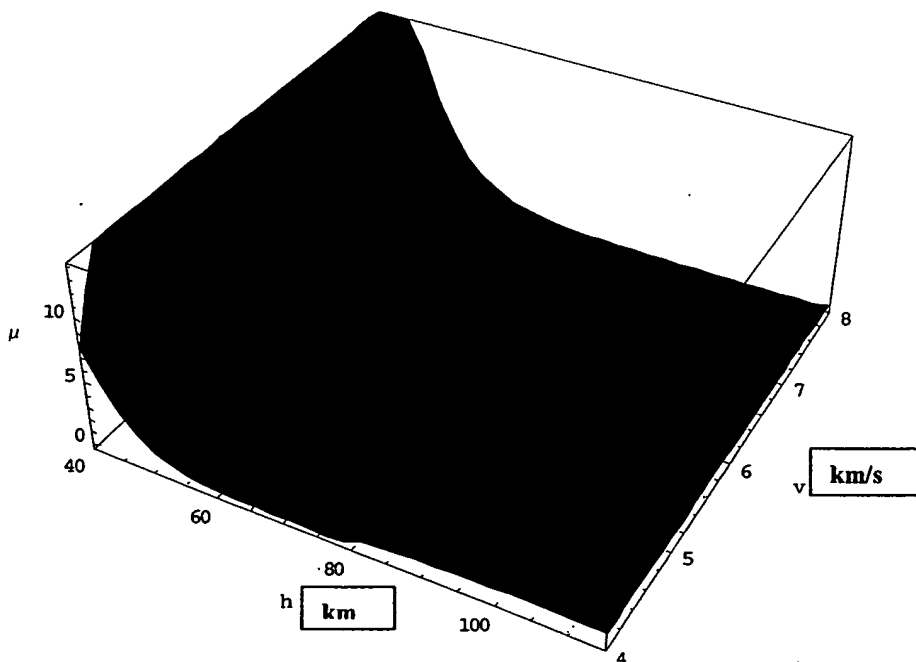


Fig. 2-3 Refractive Index v. Altitude (km) and Velocity (km/s) 421 MHz

UNCLASSIFIED

UNCLASSIFIED

The refractive index is used in classical attenuation (Appendix) to find massive attenuation at 100+ km altitude (Fig. 2-4). Note a peak at 15,000 dB near 105 km and 7+ km/s. The actual attenuation during the reentry depends on the reentry velocity v , altitude. This

allows some options for the pilot: he can typically nose up at 110 km to get some slight braking. This is however, the region that produces massive attenuation at UHF frequencies. A flight profile as Fig. 2-5 would imply the classical attenuation of Fig. 2-6.

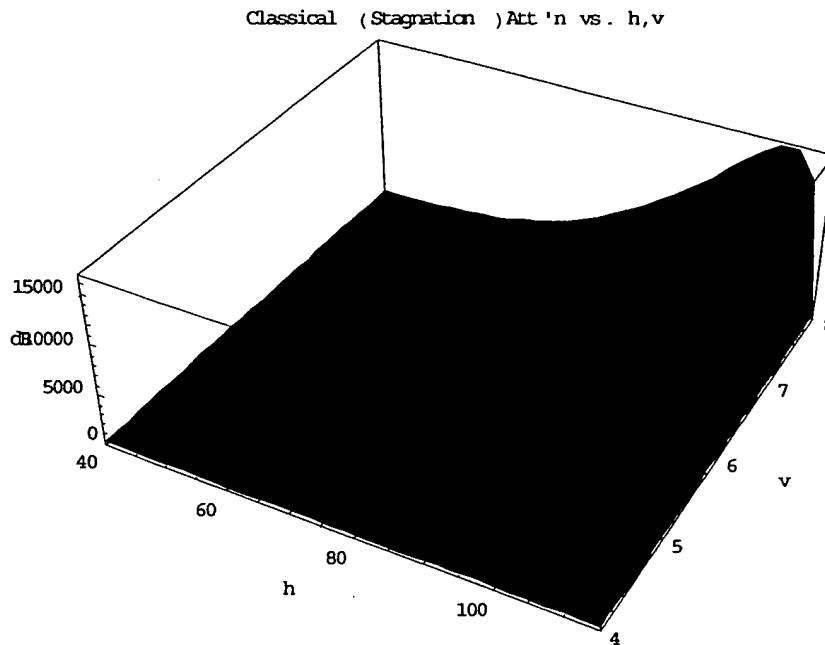


Fig. 2-4 Classical Attenuation v. Altitude (km), Velocity (km/s) 421 MHz

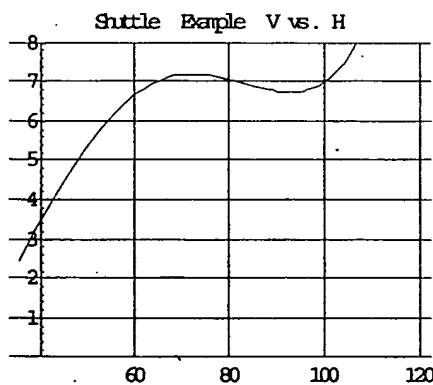


Fig. 2-5 Flight Profile; v v. h (km)

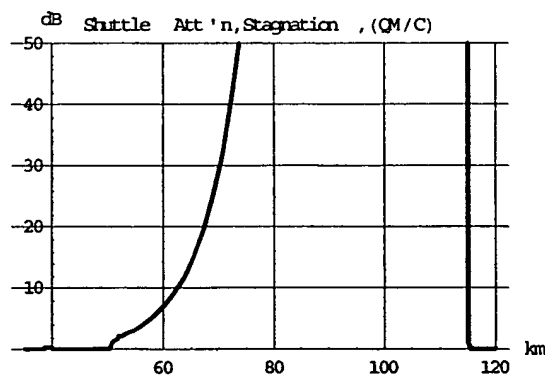


Fig. 2-6 Net Attenuation v. h (km)

The net attenuation of Fig. 2-6 actually gives some relief to the high classical attenuation of Fig. 2-4. The attenuation layers are so thin at

altitudes less than 70 km that quantum tunneling is invoked to achieve low attenuation for altitudes less than 70 km.

UNCLASSIFIED

Ka Band Communication Frequencies

The index of refraction becomes a problem at much lower altitudes for Ka band. Fig. 2-7 shows the classical attenuation v. altitude and velocity corresponding to Peng's stagnation plasma. Classical attenuation at 26 GHz is reduced to a maximum 150 dB. Only 3 dB quantum loss remains in Fig. 2-8 for the flight

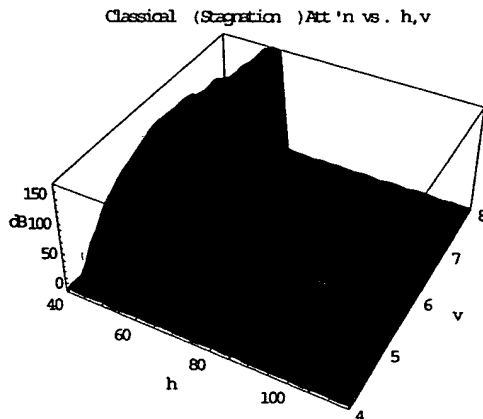


Fig. 2-7 Classical Att'n at 26 GHz

3. Attractive Surveillance Frequencies

Millimeter wave frequencies higher than 30 GHz can be at least as attractive for surveillance of the reentry vehicle as for communication. Radar discrimination increases sharply at the higher frequencies. We must of course be

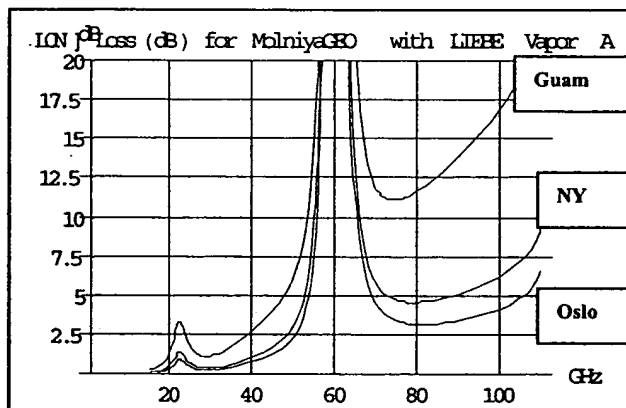


Fig. 3-1 Loss v. F at Guam, NY, Oslo Radar at Zenith; 90%

profile (Fig. 2-5). Reentry attenuation quickly fades to low levels for frequencies above 26 GHz. We might ask how high attractive frequencies might extend, and we need results for clouds, water vapor, and oxygen attenuation to address those features. This is done in the next section.

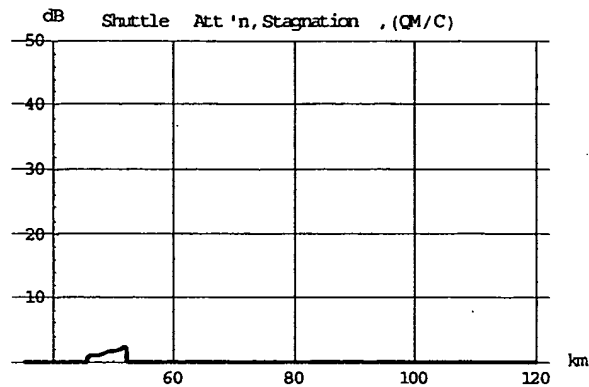


Fig. 2-8 Net Attenuation v. h at 26 GHz

concerned about atmospheric attenuation at the higher frequencies (9, 10).

Figures 3-1 and 3-2 describe 90% non rainy attenuation to Guam, New York, and Oslo. Optimum frequency from Net Loss at radar zenith for New York is indicated as 90 GHz.

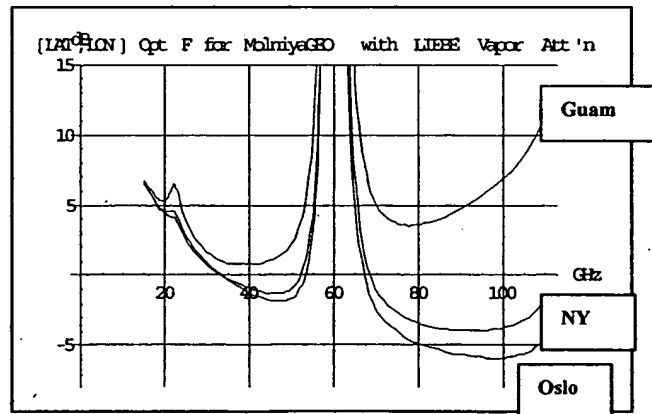


Fig. 3-2 Net Loss at Guam, NY, Oslo Radar at Zenith; 90% Att'n

UNCLASSIFIED

UNCLASSIFIED

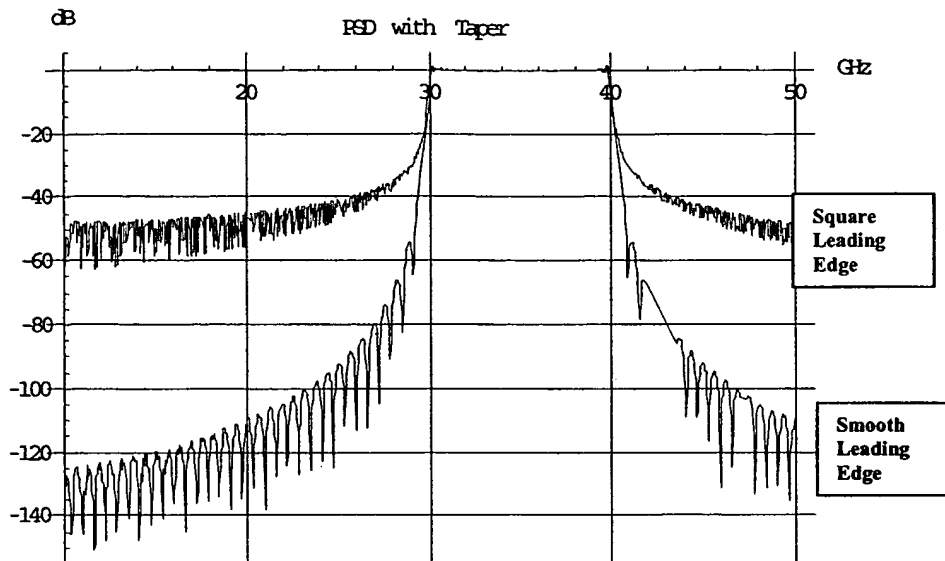


Fig. 3-3 Power Spectral Densities for 30-40 GHz Linear FM Radar $\tau=245\text{nsec}$
pgm Jun4-x2.nb

The approximate zenith net loss (Fig. 3-2) was found for radars with constant aperture and 90% non rainy attenuation conditions. Other advantages and disadvantages also apply for the 75-98 GHz band: Advantages include the higher radar resolution at the higher frequencies. Very large bandwidth can be considered, as the 10 GHz bandwidth shown for the conceptual linear FM (Chirp) radar of Fig. 3-3. Sharp spectral falloff is seen for frequencies outside the 30-40 GHz region when smooth 1.6 nsec leading and trailing edges are used (bottom curve).

Conclusions

We have extended Davies' index of refraction for plasmas in order to simulate a spacecraft reentry conditions for a wide range of altitude and velocity. We applied it to Peng's stagnation conditions for a reentry vehicle with a representative Shuttle velocity-height profile. The mean free path for the plasma was resolved with the aid of Condon and Odishaw's exponential relation to altitude. Classical attenuation was finally developed (Appendix) for the reentry vehicle as a function of altitude (h) velocity (v) and frequency (fg). Quantum tunneling relieved the classical attenuation for altitudes less than 70 km.

The reentry communication requirements emphasized frequencies greater than 26 GHz, and atmospheric attenuation requirements emphasized 26-45 GHz and 75-98 GHz. Possibilities for high radar resolution also increased at frequencies greater than 30 GHz.

Acknowledgement

David Wampler of ITT Industries provided key insights into Peng's stagnation point observations. He also discussed enhanced D Region activity (see Appendix, attached).

UNCLASSIFIED

UNCLASSIFIED

Selected References

1. F. Dirs, "The Telemetry and Communication Problem of Re-Entrant Space Vehicles," April, 1960.
2. K. Davies, Ionospheric Radio Propagation, NBS Monograph 80, 1965.
3. J. Jensen, et al, Design Guide to Orbital Flight, McGraw-Hill, NY, 1962.
4. E.U. Condon and Hugh Odishaw, Handbook of Physics, McGraw-Hill, NY, 1958.
5. Richard Dendy, Plasma Physics, Cambridge University Press, 1993.
6. Leonard I. Schiff, Quantum Mechanics, McGraw-Hill, NY, 1955.
7. Wei-Chung Peng and Henley Wu, On the Modeling of Shuttle Reentry Communication Blackout, LinCom Corp internal memo TM-8707-52, Oct. 1, 1991.
8. S. Wolfram, Mathematica, a System for Doing Mathematics by Computer, Addison Wesley, 3rd edition, 1997.
9. F. Barbaliscia, M. Boumis, A. Martellucci, "Characterization of Atmospheric Attenuation in the Absence of Rain in Europe in SHF/EHF Bands for VSAT Satcom Systems Applications," Proc. Ka Band Conference, Sorrento, Italy, Sept. 1997.
10. Paul Christopher, "Millimeter Waves for Broadband Satellite Communication, 75- 98 GHz," Proc. Ka Band Conference, Isle of Ischia, Italy, Nov. 2003.

Appendix Equation for Classical Plasma Attenuation for Reentry Vehicle

With the extended Davies' index of refraction expressed as:

$$\mu = \sqrt{\frac{\frac{4v^4}{\omega^4} - \frac{4\omega p^2 v^2}{\omega^4} + \frac{8v^2}{\omega^4} - \frac{4\omega p^2}{\omega^4} + \sqrt{\frac{4v^2 \left(\frac{4v^4}{\omega^4} + \frac{8v^2}{\omega^4} + 1 \right) \omega p^4}{\frac{4v^4}{\omega^4} - \frac{8v^2}{\omega^4} + 1}} + \left(-\frac{4v^4}{\omega^4} + \frac{4\omega p^2 v^2}{\omega^4} - \frac{8v^2}{\omega^4} + \frac{4\omega p^2}{\omega^4} - 1 \right)^2 + 4}}{\frac{4v^4}{\omega^4} - \frac{8v^2}{\omega^4} + 1}} \quad (A-1)$$

$\omega p = 56.56 \text{ Sqr}[Ne]$

The attenuation per meter through the plasma layer may be found as:

$$\text{Attenuation} = \frac{0.0000636097 \cdot 10^{\ln 2} \cdot \nu}{(\nu^2 + \omega^2) \sqrt{\frac{4v^4}{\omega^4} - \frac{4\omega p^2 v^2}{\omega^4} + \frac{8v^2}{\omega^4} - \frac{4\omega p^2}{\omega^4} + \sqrt{\frac{4v^2 \left(\frac{4v^4}{\omega^4} + \frac{8v^2}{\omega^4} + 1 \right) \omega p^4}{\frac{4v^4}{\omega^4} - \frac{8v^2}{\omega^4} + 1}} + \left(-\frac{4v^4}{\omega^4} + \frac{4\omega p^2 v^2}{\omega^4} - \frac{8v^2}{\omega^4} + \frac{4\omega p^2}{\omega^4} - 1 \right)^2 + 4}} \quad (A-2)$$

where ν = collision frequency (an exponential function of altitude; Condon and Odishaw)

(A-2)

The classical attenuation uses (A-1 and -2) and can be expressed as a much longer equation (not shown). It runs quickly in Mathematica.

D Region of Ionosphere

We omitted a key discussion of the active D Region, near 90 km altitude. High ionization levels would imply higher plasma densities than shown in Section 2. Classical attenuation at 421 MHz would have an extra hump near 90 km (compare Fig. 2-4).

UNCLASSIFIED

BEST AVAILABLE COPY

UNCLASSIFIED

Classical (Stagnation) Att'n vs. h,v

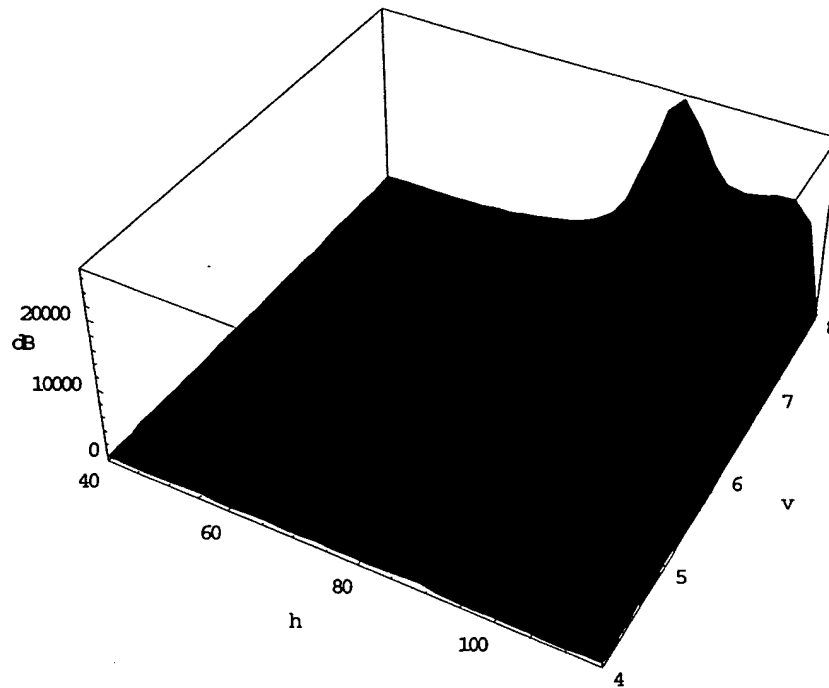


Fig. A-1 Classical Attenuation at 421 MHz v. H, V(km/s); Active D Region
Jun1DRegion-nb

UNCLASSIFIED